



UNIVERSITY OF LEEDS

This is a repository copy of *A Centralised Control Method for Tackling Unbalances in Active Distribution Grids*.

White Rose Research Online URL for this paper:  
<http://eprints.whiterose.ac.uk/129149/>

Version: Accepted Version

---

**Proceedings Paper:**

Karagiannopoulos, S, Aristidou, P [orcid.org/0000-0003-4429-0225](https://orcid.org/0000-0003-4429-0225) and Hug, G (2018) A Centralised Control Method for Tackling Unbalances in Active Distribution Grids. In: 2018 Power Systems Computation Conference (PSCC). PSCC 2018, 11-15 Jun 2018, Dublin, Ireland. IEEE . ISBN 978-1-910963-10-4

10.23919/PSCC.2018.8442493

---

This is an author produced version of a paper which has been accepted to the 20th Power Systems Computation Conference (PSCC 2018).

**Reuse**

Items deposited in White Rose Research Online are protected by copyright, with all rights reserved unless indicated otherwise. They may be downloaded and/or printed for private study, or other acts as permitted by national copyright laws. The publisher or other rights holders may allow further reproduction and re-use of the full text version. This is indicated by the licence information on the White Rose Research Online record for the item.

**Takedown**

If you consider content in White Rose Research Online to be in breach of UK law, please notify us by emailing [eprints@whiterose.ac.uk](mailto:eprints@whiterose.ac.uk) including the URL of the record and the reason for the withdrawal request.



[eprints@whiterose.ac.uk](mailto:eprints@whiterose.ac.uk)  
<https://eprints.whiterose.ac.uk/>

# A Centralised Control Method for Tackling Unbalances in Active Distribution Grids

Stavros Karagiannopoulos\*, Petros Aristidou<sup>§</sup>, Gabriela Hug\*

\* EEH - Power Systems Laboratory, ETH Zurich, Physikstrasse 3, 8092 Zurich, Switzerland

<sup>§</sup> School of Electronic and Electrical Engineering, University of Leeds, Leeds LS2 9JT, UK

Emails: {karagiannopoulos, hug}@eeh.ee.ethz.ch, p.aristidou@leeds.ac.uk

**Abstract**—Traditional distribution network operators are gradually being transformed to system operators, using modern technologies to ensure a secure and efficient operation in a rapidly changing and uncertain environment. One of their most challenging tasks is to tackle the unbalanced operation of low-voltage networks, traditionally caused by unequal loading and structural asymmetries, and exacerbated by the increased penetration of single-phase distributed energy resources. This paper proposes a centralized operation scheme based on a multi-period optimal power flow algorithm used to compute optimal set-points of the controllable distributed energy resources located in the system. The algorithm reduces the operational cost while satisfying the appropriate security and power quality constraints. Furthermore, the computational tractability of the algorithm and the incremental cost of tackling imbalances in the network are addressed. Finally, the performance of the proposed method is tested on an unbalanced low-voltage distribution network.

**Index Terms**—active distribution network, three-phase multi-period optimal power flow, backward forward sweep power flow, unbalanced operation, distributed energy resources

## I. MOTIVATION

The majority of Distributed Energy Resources (DERs) today are being installed in medium and low voltage (LV) networks, fundamentally changing the structure of modern power systems and challenging current operational and planning practices. Distribution System Operators (DSOs) are called upon to upgrade their role and use all available measures at their disposal to ensure the smooth and secure operation of their grid or support the higher voltage levels if necessary. Achieving this requires using active control measures in real-time operation and considering the flexibility of DERs in both planning and operation stages.

Many methods have been proposed for the operation of LV Distribution Networks (DNs) with high penetration of DERs. These can be classified as centralised approaches based on Optimal Power Flow (OPF) [1]–[4], distributed [5], or local [6], each requiring different levels of communication infrastructure. Typical objectives used in these methods include minimizing active power curtailment of renewables [3] and network losses [2], while satisfying power quality constraints in terms of voltages limits and thermal loading of the branches.

Most of the proposed methods in literature consider *balanced* LV DNs, mainly due to the origin of most methods in transmission network operation. However, real LV networks are *unbalanced* due to unequal spread of loads and single-phase DERs at each phase, as well as unbalanced cable/line

impedances. This can result in significant power quality problems, i.e. voltage unbalance among the phases, increased losses and reduced DER hosting capabilities. The role of an active DSO in such an unbalanced operation framework is even more challenging, and the requirements for maintaining power quality become more demanding.

The traditional techniques proposed in literature for eliminating asymmetries include distribution static synchronous compensators [7], or dynamically switching residential loads between phases [8] which are costly. Lately, new schemes have been proposed to control inverters either providing negative and zero sequence currents [9], [10] or transferring power between the phases [11]–[13] to balance the network. However, most of the references examined consider only one type of control measures and ignore the coordination potential of various active measures available to the DSO. For example, [11], [12] use only active power control of balancing inverters, ignoring reactive power or On Load Tap Changing (OLTC) transformers, while reference [13], focusing on the design of Battery Energy Storage Systems (BESS), considers only active and reactive power exchange of the inverters. Furthermore, none of the examined papers considers the unbalance requirement within an OPF framework, but they evaluate the grid conditions using power flow calculations.

This work deals with the operation of three-phase, unbalanced, LV networks with high penetration of Photovoltaic (PV) units. First, we present a centralised controller based on a multi-period OPF formulation that extends the work in [1]–[3] to optimise the operation of three-phase unbalanced DNs. We extend the OPF formulation to three-phase systems and include additional power quality (phase balancing) constraints to the original formulation. We consider a wide range of control measures, including DER active power curtailment and reactive power control, BESS control, flexible load control and setpoint selection of OLTC transformers. Finally, we investigate the incremental cost of balancing DNs through power quality constraints using different control measures.

The proposed method can be used by modern DSOs with high penetration of DERs to minimize the operational cost while satisfying the security and power quality requirements. The conclusions from this work can be used to guide the development of new grid codes, using the operational flexibility provided by active DERs to alleviate security and power quality problems and defer grid investments.

The remainder of the paper is organized as follows: Section II presents the general mathematical formulation of the OPF-based centralised controller considering the modeling of active measures and including a computationally efficient way to obtain an AC feasible solution. Section III presents the simulation results of a typical European LV grid and discusses the performance of the proposed controller. Finally, conclusions are drawn in Section IV.

## II. CENTRALISED OPF-BASED CONTROL SCHEME

Centralised control of distribution networks based on OPF formulations has gained significant attention due to advances in computational power and new theoretical developments in approximations of the non-linear AC power flow equations [1], [14], [15]. The use of the full non-convex AC power flow model becomes computationally demanding once inter-temporal constraints and large-scale DNs are considered [16], whereas the DC power flow approximation is not appropriate for DNs as the voltage magnitudes are typically not close to nominal and branch resistances are significant.

Most modern approaches are based on linear approximations of the AC power flows [5], [17], [18] and convex relaxations [15], [19], [20]. The latter, e.g. based on semi-definite relaxations [19], find globally optimal solutions of the original problem in many practical problems. However, they can also be computationally demanding and might lead to solutions which are not feasible in terms of the full AC power flow model.

Backward/Forward Sweep (BFS) is an iterative power flow solution method that exploits the radial or weakly meshed DN topology [21]. It has been used in OPF formulations [1]–[3] as it can be easily incorporated in the mathematical formulation, shows high accuracy in DNs, and leads to convex problems that can be efficiently solved. In this paper, we consider such a BFS-OPF problem formulation which can handle weakly meshed DN configurations, is computationally tractable and derives AC feasible solutions. The formulation of [2] is extended to three-phase unbalanced systems.

### A. BFS power flow

Each iteration of the BFS method consists of two sweeps (backward and forward). First, at the  $k^{th}$  iteration of time instant  $t$ , the current injected at each bus  $j$  and phase  $z \in \{a, b, c\}$ , and the current flowing in each branch are calculated by

$$I_{inj,j,z,t}^k = \left( \frac{(P_{inj,j,z,t}^f + jQ_{inj,j,z,t}^f)^*}{V_{j,z,t}^{k*}} \right), \quad j = 1, \dots, N_b \quad (1a)$$

$$I_{br,t}^k = \mathbf{BIBC} \cdot I_{inj,t}^k \quad (1b)$$

where  $P_{inj,j,z,t}^f$  and  $Q_{inj,j,z,t}^f$  are the net active and reactive power injections of each bus  $j$  (generation minus consumption);  $N_b$  is the number of buses;  $V_{j,z,t}^k$  the complex voltage of phase  $z$  at bus  $j$ ;  $I_{inj,t}^k$  and  $I_{br,t}^k$  are respectively the vectors of the three-phase bus injection and branch flow currents; and,  $\mathbf{BIBC}$  is a matrix with ones and zeros, capturing the three-phase topology of the DN (including any single-phase laterals).

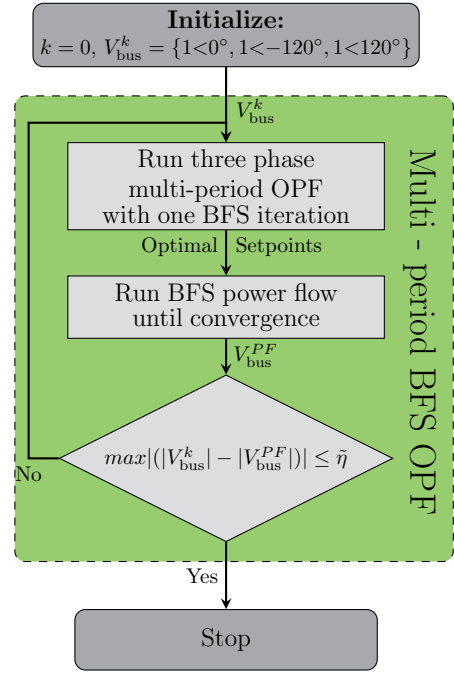


Fig. 1. Proposed multi phase BFS OPF algorithm

Then, in the forward sweep, the branch currents are used to calculate the voltage drop over all branches, using

$$\Delta V_t^{k+1} = \mathbf{BCBV} \cdot I_{br,t}^k \quad (2a)$$

and finally bus voltages are updated by

$$V_t^{k+1} = V_{slack} - \Delta V_{tap} \cdot \rho_t + \Delta V_t^{k+1} \quad (2b)$$

where  $\Delta V_t^{k+1}$  is the vector of voltage drops over all branches and phases;  $\mathbf{BCBV}$  is a matrix with the complex impedance of the lines as elements (including mutual coupling);  $V_{slack}$  is the three-phase voltage in per unit at the slack bus (here assumed to be  $\{1 < 0^\circ, 1 < -120^\circ, 1 < 120^\circ\}$ );  $\Delta V_{tap}$  is the voltage magnitude change caused by one tap action of the OLTC transformer and assumed constant for all taps for simplicity; and,  $\rho_t$  is an integer value defining the position of the OLTC tap.

The BFS procedure defined by (1) and (2) is repeated until the norm of the voltage difference computed in two consecutive iterations is smaller than a given threshold.

### B. BFS in an OPF framework

In an OPF framework, a single iteration of the BFS equations (1) and (2) is embedded in the optimization formulation to replace the non-convex, exact, AC power flow equations. After we obtain the optimal OPF setpoints, we perform an exact BFS power flow to derive an AC feasible operating point (in contrast to [1] where only one BFS iteration is used), whose solution for the lateral voltages will be used in the next OPF iteration. The loop is repeated until convergence in terms of voltage magnitude mismatch is reached. This approach is summarized in Fig. 1 and detailed in [2].

### C. Mathematical Formulation of the centralised OPF scheme

1) *Objective function*: The objective function includes the cost of DER control and network losses over all network nodes ( $N_b$ ), phases ( $z$ ) and branches ( $N_{br}$ ) for the entire time horizon ( $N_{hor}$ )

$$\begin{aligned} \min_{\mathbf{u}} \sum_{t=1}^{N_{hor}} \left\{ \sum_{z \in \{a,b,c\}} \sum_{j=1}^{N_b} \left( C_P \cdot P_{\text{curt},j,z,t} + C_Q \cdot Q_{\text{ctrl},j,z,t} \right) \right. \\ \left. + \sum_{i=1}^{N_{br}} C_P \cdot P_{\text{loss},i,z,t} \right\} \cdot \Delta t \\ + C_H \cdot \left( \|\varepsilon_V\|_{\infty} + \|\varepsilon_I\|_{\infty} + \|\varepsilon_{VUF}\|_{\infty} \right) \end{aligned} \quad (3)$$

where  $\mathbf{u}$  is the vector of active control measures (different control measures are considered later on) and  $\Delta t$  is the length of each time period. The curtailed power of the Distributed Generators (DGs) connected at phase  $z$ , at node  $j$  and time  $t$  is given by  $P_{\text{curt},j,z,t} = P_{g,j,z,t}^{\text{max}} - P_{g,j,z,t}^f$ , where  $P_{g,j,z,t}^{\text{max}}$  is the maximum available active power and  $P_{g,j,z,t}^f$  is the actual infeed. The use of the reactive power support  $Q_{g,j,z,t}^f$  for each DG at phase  $k$  of node  $j$  and time  $t$  is minimized by including the term  $Q_{\text{ctrl},j,z,t} = |Q_{g,j,z,t}^f|$  in the objective function. The coefficients  $C_P$  and  $C_Q$  represent, respectively, the DG cost of curtailing active power and providing reactive power support. Selecting  $C_Q \ll C_P$  prioritizes the use of reactive power control over active power curtailment. The losses considering all branches and mutual coupling at time  $t$  are calculated by  $P_{\text{loss},i,z,t} = |I_{br,i,z,t}|^2 \cdot R_{br,i,z}$ , where  $|I_{br,i,z,t}|$  is the magnitude of the current flow and  $R_{br,i,z}$  its resistance. Finally,  $C_H$  is a large cost associated with violating the security and power quality constraints. It is used, in conjunction with the variables ( $\varepsilon_V, \varepsilon_I, \varepsilon_{VUF}$ ) to relax respectively the voltage, thermal or balancing constraints and avoid infeasibility. The infinite norm is minimized over all time instances, phases, cables, and buses accordingly.

It should be noted that while the active and reactive control costs ( $C_P, C_Q$ ) have a real monetary meaning for the DSO, the cost  $C_H$  is used only to avoid infeasibility during the operation. When one of these limits is binding, the output of the overall objective function loses the real monetary meaning (unless the cost of violating the security and power quality constraints can be quantified and monetized – e.g., faster component degradation, higher losses, etc.).

2) *Power balance constraints*: The power injection equations at every node  $j$ , phase  $z$  and time step  $t$  are given by

$$P_{\text{inj},j,z,t}^f = P_{g,j,z,t}^f - P_{\text{fllex},j,z,t}^f - (P_{B,j,z,t}^{\text{ch}} - P_{B,j,z,t}^{\text{dis}}), \quad (4a)$$

$$Q_{\text{inj},j,z,t}^f = Q_{g,j,z,t}^f - P_{\text{flflex},j,z,t}^f \cdot \tan(\phi_{\text{load}}). \quad (4b)$$

For each node  $j$ , phase  $z$  and time step  $t$ ,  $P_{g,j,z,t}^f$  and  $Q_{g,j,z,t}^f$  are the active and reactive power injections of the DGs;  $P_{\text{flflex},j,z,t}^f$  and  $P_{\text{flflex},j,z,t}^f \cdot \tan(\phi_{\text{load}})$  are the active and reactive node demands (after control), with  $\cos(\phi_{\text{load}})$  being the power factor of the load; and,  $P_{B,j,z,t}^{\text{ch}}$  and  $P_{B,j,z,t}^{\text{dis}}$  are respectively the charging and discharging power of the BESS.

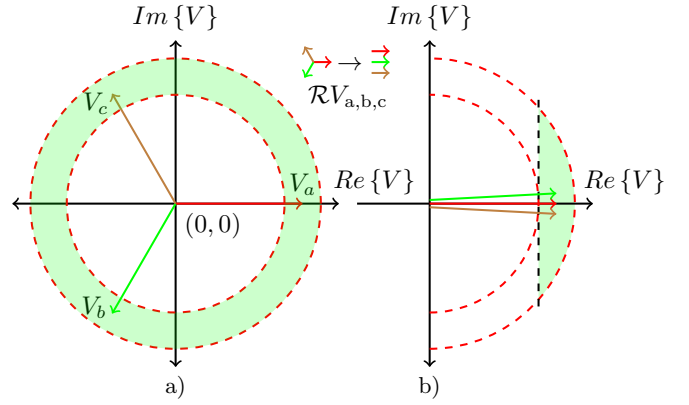


Fig. 2. Reformulation of voltage magnitude constraints

3) *Power flow constraints*: As explained in the previous section, a single iteration of the BFS power flow problem considering the OLTC capabilities, detailed in Section II-A, is used for the power flow constraints. That is ( $j = 1, \dots, N_b$ ,  $z \in \{a, b, c\}$ ):

$$I_{\text{inj},j,z,t} = \left( \frac{(P_{\text{inj},j,z,t}^f + jQ_{\text{inj},j,z,t}^f)^*}{V_{j,z,t}^*} \right) \quad (5)$$

$$I_{br,t} = \mathbf{BIBC} \cdot I_{\text{inj},t} \quad (6)$$

$$\Delta \mathbf{V}_t = \mathbf{BCBV} \cdot I_{br,t} \quad (7)$$

$$\mathbf{V}_t = \mathbf{V}_{\text{slack}} - \Delta \mathbf{V}_{\text{tap}} \cdot \rho_t + \Delta \mathbf{V}_t \quad (8)$$

$$\rho_{\min} \leq \rho_t \leq \rho_{\max}, \quad (9)$$

where the parameters ( $\rho_{\min}, \rho_{\max}$ ) are respectively the minimum and maximum tap positions of the OLTC transformer.

4) *Thermal loading and voltage constraints*: The constraint for the current magnitude for all branches  $i$  and phase  $z$  at time  $t$  is given by

$$|I_{br,i,z,t}| \leq I_{i,z,\max} + \varepsilon_{I,i,z,t} \quad (10a)$$

$$\varepsilon_{I,i,z,t} \geq 0 \quad (10b)$$

where  $I_{br,i,z,t}$  is the branch current from (6);  $I_{i,z,\max}$  is the maximum thermal limit; and,  $\varepsilon_{I,i,z,t}$  is used to relax the constraint when the thermal constraints cannot be met.

Similarly, the voltage constraints are given by

$$V_{\min} - \varepsilon_{V,j,z,t} \leq |V_{j,z,t}| \leq V_{\max} + \varepsilon_{V,j,z,t} \quad (11a)$$

$$\varepsilon_{V,j,z,t} \geq 0 \quad (11b)$$

where ( $V_{\max}, V_{\min}$ ) are respectively the upper and lower acceptable voltage limits and  $\varepsilon_{V,j,z,t}$  is used to relax the constraint when the voltage constraints cannot be met.

It can be seen from Fig. 2a that the constraint (11a) is non-convex. We rewrite it as the convex formulation given by

$$\begin{cases} |\mathcal{R}V_{j,t}| \leq V_{\max} + \varepsilon_{V,j,t} \\ Re\{\mathcal{R}V_{j,t}\} \geq V_{\min} - \varepsilon_{V,j,t} \end{cases} \quad (12)$$

and shown graphically in Fig. 2b. This corresponds to first rotating the three voltage phases  $\{a, b, c\}$  by  $\mathcal{R} = -\{1 < 0^\circ, 1 < -120^\circ, 1 < 120^\circ\}$  so that they lie close to the reference axis  $0^\circ$  and defining the same feasible space for each of the

three phases. The arc can then be approximated by piecewise linear segments in order to approximate the second order cone (see upper part of (12)) with a set of linear constraints, maintaining convexity.

5) *Balancing constraint*: Different ways have been proposed to define and calculate the voltage phase unbalance [22]. The IEC definition of the Voltage Unbalance Factor (VUF) is given by  $VUF(\%) = 100\% \frac{|V_-|}{|V_+|}$ , where  $V_-$ ,  $V_+$  are respectively the negative and positive voltage sequence derived by symmetrical component analysis.

Trying to limit the VUF in an OPF framework for each bus  $i$  and time  $t$ , will result in the non-convex constraint  $VUF_{j,t}(\%) \leq VUF_{MAX}$ , where  $VUF_{MAX}$  is the acceptable voltage unbalance factor, e.g. 2% for 95% of the week according to EN50160 [23]. To avoid this non-convexity, we approximate VUF by the negative voltage sequence, assuming the positive voltage sequence is very close to 1.0 when expressed in per-unit [24]. Therefore, the following balancing constraint is used

$$VUF_{j,t}(\%) \approx 100 \cdot |V_{-j,t}^{k*}| \leq VUF_{MAX} + \varepsilon_{VUF,j,t} \quad (13a)$$

$$\varepsilon_{VUF,j,t} \geq 0 \quad (13b)$$

where  $\varepsilon_{VUF,j,t}$  is used to relax the constraint when the balancing constraints cannot be met and  $V_{-j,t}^{k*}$  is the negative voltage sequence according to the symmetrical component analysis given by

$$\begin{bmatrix} V_{0,j,t}^{k+1*} \\ V_{-j,t}^{k+1*} \\ V_{+j,t}^{k+1*} \end{bmatrix} = \frac{1}{3} \begin{bmatrix} 1 & 1 & 1 \\ 1 & e^{j120^\circ} & e^{-j120^\circ} \\ 1 & e^{-j120^\circ} & e^{j120^\circ} \end{bmatrix} \begin{bmatrix} V_{j,a,t}^{k+1} \\ V_{j,b,t}^{k+1} \\ V_{j,c,t}^{k+1} \end{bmatrix}. \quad (14)$$

6) *Active measures constraints*:

a) *DG limits*: In this work, we consider inverter-based DGs such as PVs. The limits are given by

$$P_{g,j,z,t}^{\min} \leq P_{g,j,z,t}^f \leq P_{g,j,z,t}^{\max} \quad (15a)$$

$$-\tan(\phi_{\max})P_{g,j,z,t}^f \leq Q_{g,j,z,t}^f \leq \tan(\phi_{\max})P_{g,j,z,t}^f, \text{ or,} \quad (15b)$$

$$-\tan(\phi_{\max})P_{g,j,z,t}^{\min} \leq Q_{g,j,z,t}^f \leq \tan(\phi_{\max})P_{g,j,z,t}^{\max} \quad (15c)$$

where  $P_{g,j,z,t}^{\min}$  and  $P_{g,j,z,t}^{\max}$  are the upper and lower limits for active DG power at each node  $j$ , phase  $z$  and time  $t$ . These limits vary depending on the type of the DG and the control schemes implemented. Usually, small DGs have technical or regulatory [25] limitations on the power factor they can operate at or reactive power they can produce. Here, we consider two variants: the reactive power constraint of (15b) limits the reactive power output as a function of the actual active power injection and the maximum power factor  $\cos(\phi_{\max})$ ; while, in (15c), the reactive power limit is independent of the active power injection and limited by a constant maximum value.

b) *Controllable loads*: We consider flexible loads which can shift a fixed amount of power in time. The behavior of the loads at each controllable node  $j$  and phase  $z$  is given by

$$P_{\text{flex},j,z,t}^f = P_{l,j,z,t}^f + n_{j,z,t} \cdot P_{\text{shift},j,z} \quad (16a)$$

$$\sum_{t=1}^{N_{hor}} n_{j,z,t} = 0, \quad (16b)$$

where  $P_{\text{flex},j,z,t}^f$  is the final controlled active demand at node  $j$  of phase  $z$  and time  $t$ ,  $P_{\text{shift},j,z}$  is the constant shiftable load at node  $j$  and  $n_{j,z,t} \in \{-1, 0, 1\}$  is an integer variable indicating an increase or a decrease of the load when shifted from the known initial demand  $P_{l,j,z,t}^f$ . Constraint (16b) assures that the final total daily energy demand is maintained.

c) *Battery Energy Storage Systems*: Finally, the constraints related to the BESS are given as

$$SoC_{\min}^{\text{bat}} \cdot E_{\text{cap},j,z}^{\text{bat}} \leq E_{j,z,t}^{\text{bat}} \leq SoC_{\max}^{\text{bat}} \cdot E_{\text{cap},j,z}^{\text{bat}}, \quad (17a)$$

$$E_{j,z,1}^{\text{bat}} = E_{\text{start}}, \quad (17b)$$

$$E_{j,z,t}^{\text{bat}} = E_{j,z,t-1}^{\text{bat}} + \left( \eta_{\text{bat}} \cdot P_{B,j,z,t}^{\text{ch}} - \frac{P_{B,j,z,t}^{\text{dis}}}{\eta_{\text{bat}}} \right) \cdot \Delta t, \quad (17c)$$

$$P_{B,j,z,t}^{\text{ch}} \geq 0, \quad P_{B,j,z,t}^{\text{dis}} \geq 0, \quad (17d)$$

$$P_{B,j,z,t}^{\text{ch}} + P_{B,j,z,t}^{\text{dis}} \leq \max(P_{B,j,z,t}^{\text{ch}}, P_{B,j,z,t}^{\text{dis}}), \quad (17e)$$

where  $E_{\text{cap},j,z}^{\text{bat}}$  is the installed BESS capacity connected at phase  $z$  at node  $j$ ;  $SoC_{\min}^{\text{bat}}$ ,  $SoC_{\max}^{\text{bat}}$  are the fixed minimum and maximum per unit limits for the battery state of charge; and,  $E_{j,z,t}^{\text{bat}}$  is the available energy at node  $j$ , phase  $z$  and time  $t$ . The initial energy content of the BESS in time period 1 is given by  $E_{\text{start}}$ , and (17c) updates the energy in the storage at each time step  $t$  based on the BESS efficiency  $\eta_{\text{bat}}$ , time interval  $\Delta t$  and the charging and discharging power of the BESS  $P_{B,j,z,t}^{\text{ch}}$  and  $P_{B,j,z,t}^{\text{dis}}$ . The charging and discharging power are defined as positive according to (17d). Equation (17e) ensures that the BESS is not charging and discharging at the same time.

### III. CASE STUDY - RESULTS

In this section, we first describe the three-phase unbalanced LV DN used in this work and the performance indices showing the effectiveness of the proposed control method. Then, we show through various scenarios the impact of considering balancing constraints in the DN operation and the cost of using a combination of active measures.

The implementation was done in MATLAB using YALMIP [26] as the modeling layer and Gurobi [27] as the solver. The results were obtained on an Intel Core i7-2600 CPU and 16 GB of RAM.

#### A. Network description - Case study setup

In this work, we use a typical European radial LV grid, detailed in [28] and depicted in Fig. 3, to demonstrate the proposed methodology. Table I contains the phase impedance of the underground cables after Kron reduction. The neutral is assumed to be earthed in several points, and due to the short lengths of cables the capacitance is neglected.

In order to simulate unbalanced conditions, we distribute the load and PV panels unevenly. More specifically, the total load taken from [28] is split in 25%, 60%, and 15% among the three phases. The installed PV capacity, is set to  $S_{\text{rated}}^{\text{PV}} = 28\%$  of the total maximum load of the entire feeder to the PV nodes = [12, 16, 17, 18, 19], and is shared on average by 15%, 15% and 70% among the three phases. Furthermore, we consider BESS at the PV nodes of capacity equal to  $\frac{1}{2} S_{\text{rated}}^{\text{PV}}$  kWh, where  $S_{\text{rated}}^{\text{PV}}$  is the rated power of the PV unit at that particular node, and

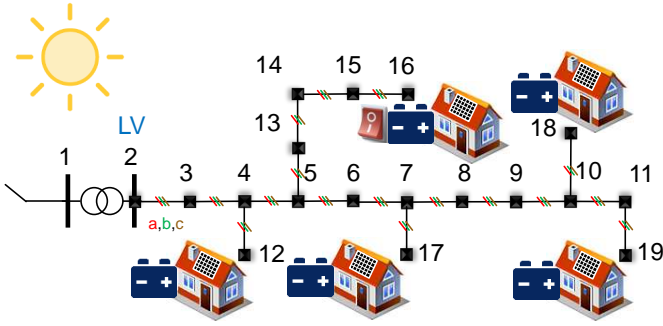


Fig. 3. Cigre LV grid.

a flexible load of 5 kW connected at phase C of Node 16, whose total daily energy consumption needs to be maintained constant. Please note that we assume single-phase connections for both the loads and the PV panels.

The operational costs are assumed to be  $C_p = 0.1 \frac{\text{CHF}}{\text{kWh}}$  and  $C_Q = 0.01 \cdot C_p$ . The BESS, CL, and OLTC costs are considered in the planning stage [3] and thus, their use does not incur any operational cost to the DNO. Finally,  $C_H = 1000 \cdot C_p$  to be used to avoid infeasible solutions.

### B. Performance indices

In order to quantify the benefit from the control measures, we use the normalized curtailed PV production and reactive power utilization (consumption/production) as given by

$$m_P = \frac{\sum_{t=1}^{N_{\text{hor}}} \sum_{j=1}^{N_b} \sum_{z \in \{a,b,c\}} P_{\text{curt},j,z,t}}{\sum_{t=1}^{N_{\text{hor}}} \sum_{j=1}^{N_b} \sum_{z \in \{a,b,c\}} P_{g,j,z,t}^{\text{max}}} \quad (18)$$

$$m_Q = \frac{\sum_{t=1}^{N_{\text{hor}}} \sum_{j=1}^{N_b} \sum_{z \in \{a,b,c\}} |Q_{g,j,z,t}^f|}{\sum_{t=1}^{N_{\text{hor}}} \sum_{j=1}^{N_b} \sum_{z \in \{a,b,c\}} |Q_{g,j,z,t}^{\text{max}}|} \quad (19)$$

where  $Q_g^{\text{max}}$  is the maximum potential injection or absorption of reactive power according to the inverter capabilities. In addition, the  $VUF$  introduced in Section II-C5 is used to depict the power quality in terms of voltage unbalance.

### C. Impact of considering balancing constraint

In order to highlight the importance of considering the balancing constraint presented in Section II-C5, we consider the test system with only the PV panels and no other controllable sources in three different scenarios:

TABLE I  
PHASE IMPEDANCE MATRICES OF UNDERGROUND LINES [28]

| Conductor  | Phase impedance matrix after Kron reduction [ $\Omega/\text{km}$ ] |                |                |                |
|------------|--|----------------|----------------|----------------|
|            | A  | B              | C              |                |
| UG1 / 3-ph | A  | 0.287 + j0.167 | 0.121 + j0.110 | 0.125 + j0.070 |
|            | B  | 0.121 + j0.110 | 0.279 + j0.203 | 0.121 + j0.110 |
|            | C  | 0.125 + j0.070 | 0.121 + j0.110 | 0.287 + j0.167 |
| UG3 / 3-ph | A  | 1.152 + j0.458 | 0.321 + j0.390 | 0.330 + j0.359 |
|            | B  | 0.321 + j0.390 | 1.134 + j0.477 | 0.321 + j0.390 |
|            | C  | 0.330 + j0.359 | 0.321 + j0.390 | 1.152 + j0.458 |

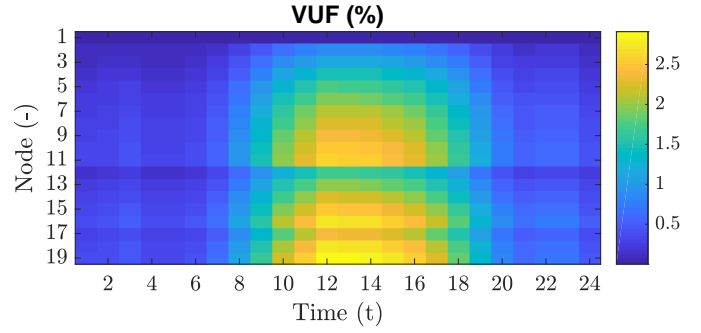


Fig. 4. Daily voltage unbalance factor at all nodes without any control.

- Case 0: This is the base case. For each time step, an AC PF solution is performed *without any control*. PV panels are operating with a unity power factor;
- Case 1: The centralized OPF-based control is used but *without the balancing constraint*. The PV panels have capabilities for active power curtailment and reactive power control with  $\cos\phi_{\text{max}} = 0.9$ ;
- Case 2: The centralized OPF-based control is used with the balancing constraint and  $VUF_{\text{MAX}} = 2\%$ .

Figure 4 shows the  $VUF$  for Case 0 on all buses throughout the day. It can be seen that the unbalanced conditions are more pronounced during the time of higher PV generation.

Figure 5 and 6 show respectively the three phase voltages and  $VUF$  values for Node 16 in the system. In all three cases, phase C shows higher voltages due to higher single phase PV generation and lower load. We observe that without control (Case 0) this phase experiences overvoltages (dashed black line above 1.1 p.u which is defined as the upper limit according to [23]). On the other hand, Case 1 succeeds in mitigating the overvoltage issue by consuming reactive power and curtailing active power from the single phase PV unit. As a result, the voltage at this phase is reduced to acceptable values (solid blue line). The other phases are influenced through the mutual coupling of the cables and different optimal setpoints at these phases. However, the  $VUF$  value is still unacceptable. By curtailing more active power at phase C and modifying also the voltages at the other phases through reactive power control, Case 3 succeeds in mitigating both the overvoltage and the phase unbalance issues.

### D. Cost of phase balancing considering a mix of active control measures

In this part, we quantify the additional cost and use of active measures when considering the balancing constraint, varying the set of available active measures.

Figure 7 summarizes the total costs incurred to the DSO with and without using the phase balancing constraint for the different active measures (each point in the figure includes all the previous measures and plus the additional one indicated). Overall, the operational cost decreases with more available measures, since other control measures are employed to satisfy the network constraints (instead of active power curtailment which is the most expensive option). It can be also observed that apart from the first case, where only active power

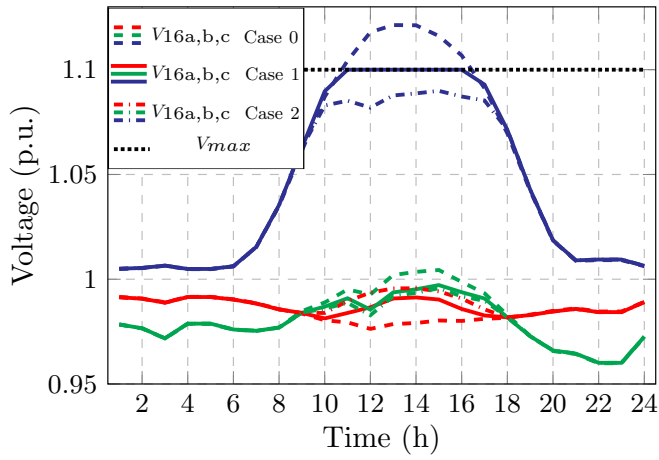


Fig. 5. Daily three-phase voltages at Node 16 without any control (Case 0), using OPF with (Case 2) and without (Case 1) considering the balancing constraint.

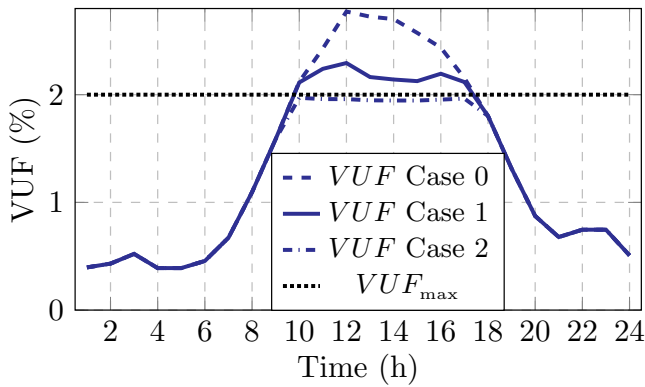


Fig. 6. Daily voltage unbalance factor at Node 16 without any control (Case 0), using OPF with (Case 2) and without (Case 1) considering the balancing constraint.

curtailment is allowed, the incremental cost of bringing the  $VUF$  within the acceptable limits is small. Thus, by allowing reactive power control in LV grids we observe lower active power curtailment to mitigate voltage issues, the losses can be optimized, and the grid shows acceptable unbalances with marginal additional cost. It should be reminded that in this work the use of BESS, CL and OLTC do not incur additional cost to the DSO in the operation phase, and thus, they lead to a further total cost decrease. Their overall cost is assumed to be accounted for in the planning stage similar to [3].

Table II summarizes the performance indices introduced in Section III-B with and without considering the balancing constraint. It can be seen that balancing the phases using only active power curtailment (APC) is costly as indicated by the large increase in  $m_P$  from Case 1 to Case 2 for the column of APC only. At the same time, when other active measures are considered, the cost of balancing is comparable in both two cases. The most significant increase is observed in the  $m_Q$  index of Case 2 (2-4 times), indicating the increased use of reactive power for balancing. This control measure is cheap, and can influence the local voltages in order to reduce unbalances. Finally, considering the  $VUF_{MAX}$  index, we can

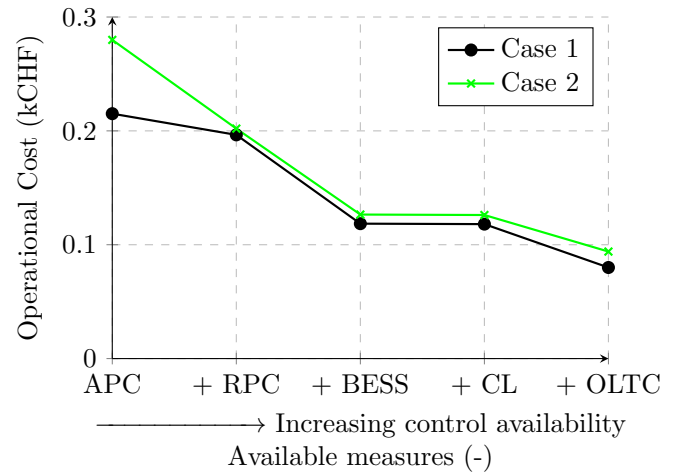


Fig. 7. Weekly operational costs for different sets of active measures. APC = Active Power Curtailment, RPC = Reactive Power Control, BESS = Battery Energy Storage System, CL = Controllable Load, OLTC = On Load Tap Changing transformer

TABLE II  
PERFORMANCE INDICES WITH AND WITHOUT CONSIDERING THE BALANCING CONSTRAINT

| PI              | Case | APC    | +▼RPC | +■RPC | +BESS | +CL   | +OLTC |
|-----------------|------|--------|-------|-------|-------|-------|-------|
| $m_P(\%)$       | 1    | 8.519  | 7.558 | 7.557 | 3.928 | 3.915 | 2.078 |
|                 | 2    | 11.687 | 7.745 | 7.732 | 4.179 | 4.161 | 2.577 |
| $m_Q(\%)$       | 1    | 0      | 6.38  | 5.75  | 8.02  | 8.91  | 18.69 |
|                 | 2    | 0      | 22.23 | 20.96 | 28.66 | 28.66 | 41.81 |
| $VUF_{MAX}(\%)$ | 1    | 2.294  | 2.664 | 2.695 | 2.761 | 2.804 | 3.017 |
|                 | 2    | 1.976  | 1.996 | 2.005 | 1.994 | 1.997 | 2.001 |

observe that the approximation of (13a) is reasonable, since the maximum derived values are very close to the desired limit of 2%.

#### E. Sensitivity of operational cost with respect to $VUF_{MAX}$

In this subsection, we vary the  $VUF_{MAX}$  in order to investigate the impact on the operational cost. Furthermore, we compare the two different reactive power controls of the PV inverters to quantify the benefit of having higher reactive power flexibility in terms of cost savings.

Figure 8 shows the weekly DSO costs for different  $VUF_{MAX}$  values and two types of PV inverter reactive power capability: the "triangular" limitations of (15b) with solid lines and the "rectangular" limitations of (15c) with dashed lines. We have already observed earlier (Fig. 7) that setting the  $VUF_{MAX}$  to 2% leads to a very small cost increase compared to the case without balancing constraints except for the case APC only. However, further decreasing the  $VUF_{MAX}$  leads to a cost increase of more than 50% for  $VUF_{MAX} = 1.5\%$ , and 200% (resp. 300%) for  $VUF_{MAX} = 1\%$  (resp.  $VUF_{MAX} = 0.75\%$ ), with the more restrictive (triangular) PV inverter reactive capabilities.

Finally, allowing the inverters to operate in the "rectangular" region of their  $P-Q$  capability curve, leads to smaller costs for all the different  $VUF_{MAX}$  values. The benefit is larger for smaller  $VUF_{MAX}$  values where more control effort is needed to satisfy the balancing constraint.

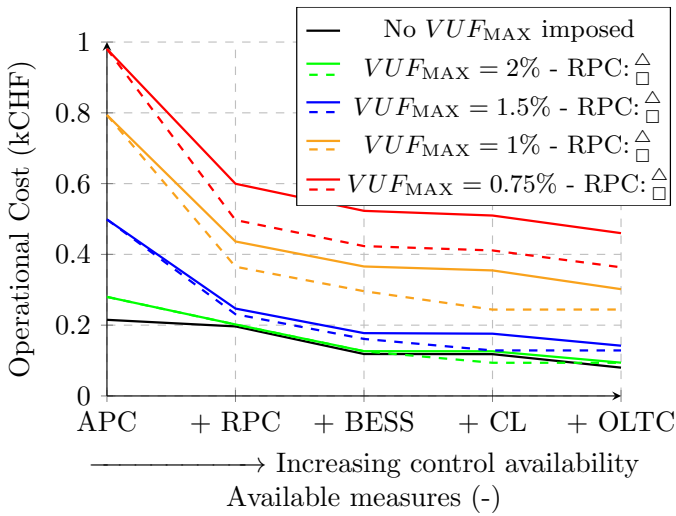


Fig. 8. Weekly operational cost for various acceptable limits of maximum voltage unbalance factor and different sets of active measures.

#### IV. CONCLUSION

With the advent of cheap and reliable communication and computation capabilities in LV DNs, the use of centralized, OPF-based control schemes to operate the system will become more attractive. Such schemes allow to optimize system operation while ensuring its security. However, the increased penetration of single-phase DERs in DNs increases the concerns about maintaining a balanced system operation to boost power quality. In this paper, we have shown that such power quality considerations can be easily introduced in this control framework by extending the OPF formulation to capture the unbalanced behaviour of three-phase DNs and introducing appropriate power quality constraints. The cost associated with the balancing of DNs has been quantified for different acceptable voltage unbalance factors, showing that reactive power control is the most appropriate control measure which can reduce voltage unbalances without increasing significantly the operational cost.

#### REFERENCES

- [1] P. Fortenbacher, M. Zellner, and G. Andersson, "Optimal sizing and placement of distributed storage in low voltage networks," in *Proceedings of the 19th Power Systems Computation Conference (PSCC), Genova*, Jun 2016.
- [2] S. Karagiannopoulos, P. Aristidou, L. Roald, and G. Hug, "Operational Planning of Active Distribution Grids under Uncertainty," in *IREP2017, X Bulk Power Systems Dynamics and Control Symposium, Espinho*, Aug 2017.
- [3] S. Karagiannopoulos, P. Aristidou, and G. Hug, "Co-optimisation of Planning and Operation for Active Distribution Grids," in *Proceedings of the 12th IEEE Power and Energy Society PowerTech Conference, Manchester*, Jun 2017.
- [4] S. Karagiannopoulos, P. Aristidou, and G. Hug, "Hybrid approach for planning and operating active distribution grids," *IET Generation, Transmission & Distribution*, pp. 685–695, Feb 2017.
- [5] S. Bolognani and S. Zampieri, "A distributed control strategy for reactive power compensation in smart microgrids," *IEEE Transactions on Automatic Control*, vol. 58, no. 11, pp. 2818–2833, Nov. 2013.
- [6] E. Demirok, P. C. González, K. H. B. Frederiksen, D. Sera, P. Rodriguez, and R. Teodorescu, "Local reactive power control methods for overvoltage prevention of distributed solar inverters in low-voltage grids," *IEEE Journal of Photovoltaics*, vol. 1, no. 2, pp. 174–182, 2011.

- [7] Y. Xu, L. Tolbert, J. Kueck, and D. Rizy, "Voltage and current unbalance compensation using a static var compensator," *IET Power Electronics*, vol. 3, no. 6, p. 977, 2010.
- [8] F. Shahnia, P. J. Wolfs, and A. Ghosh, "Voltage unbalance reduction in low voltage feeders by dynamic switching of residential customers among three phases," *IEEE Transactions on Smart Grid*, vol. 5, no. 3, pp. 1318–1327, 2014.
- [9] X. Su, M. A. S. Masoum, and P. J. Wolfs, "Optimal PV Inverter Reactive Power Control and Real Power Curtailment to Improve Performance of Unbalanced Four-Wire LV Distribution Networks," *IEEE Transactions on Sustainable Energy*, vol. 5, no. 3, pp. 967–977, Jul 2014.
- [10] R. Caldon, M. Coppo, and R. Turri, "Distributed voltage control strategy for LV networks with inverter-interfaced generators," *Electric Power Systems Research*, vol. 107, pp. 85–92, Feb 2014.
- [11] S. Weckx and J. Driesen, "Load Balancing With EV Chargers and PV Inverters in Unbalanced Distribution Grids," *IEEE Transactions on Sustainable Energy*, vol. 6, no. 2, pp. 635–643, Apr 2015.
- [12] S. Weckx, C. Gonzalez, and J. Driesen, "Reducing grid losses and voltage unbalance with PV inverters," in *2014 IEEE PES General Meeting — Conference & Exposition*, no. October. IEEE, Jul 2014.
- [13] F. Geth, J. Tant, R. Belmans, and J. Driesen, "Balanced and unbalanced inverter strategies in battery storage systems for low-voltage grid support," *IET Generation, Transmission & Distribution*, vol. 9, no. 10, pp. 929–936, Jul 2015.
- [14] E. Dall'Anese, K. Baker, and T. Summers, "Chance-Constrained AC Optimal Power Flow for Distribution Systems with Renewables," *IEEE Transactions on Power Systems*, 2017.
- [15] E. Dall'Anese, S. V. Dhople, B. B. Johnson, and G. B. Giannakis, "Optimal Dispatch of Residential Photovoltaic Inverters Under Forecasting Uncertainties," *IEEE Journal of Photovoltaics*, vol. 5, no. 1, pp. 350–359, Jan 2015.
- [16] S. Karagiannopoulos, P. Aristidou, A. Ulbig, S. Koch, and G. Hug, "Optimal planning of distribution grids considering active power curtailment and reactive power control," *IEEE Power and Energy Society General Meeting*, 2016.
- [17] M. D. Sankur, R. Dobbe, E. Stewart, D. S. Callaway, and D. B. Arnold, "A Linearized Power Flow Model for Optimization in Unbalanced Distribution Systems," Jun 2016. [Online]. Available: <http://arxiv.org/abs/1606.04492>
- [18] S. V. Dhople, S. S. Guggilam, and Y. C. Chen, "Linear approximations to AC power flow in rectangular coordinates," in *2015 53rd Annual Allerton Conference on Communication, Control, and Computing (Allerton)*. IEEE, Sep. 2015.
- [19] J. Lavaei and S. H. Low, "Zero duality gap in optimal power flow problem," *IEEE Transactions on Power Systems*, vol. 27, no. 1, pp. 92–107, 2012.
- [20] D. K. Molzahn and I. A. Hiskens, "Sparsity-Exploiting Moment-Based Relaxations of the Optimal Power Flow Problem," *IEEE Transactions on Power Systems*, vol. 30, no. 6, pp. 3168–3180, Nov 2015.
- [21] J. H. Teng, "A direct approach for distribution system load flow solutions," *IEEE Transactions on Power Delivery*, vol. 18, no. 3, pp. 882–887, 2003.
- [22] P. Pillay and M. Manyage, "Definitions of Voltage Unbalance," *IEEE Power Engineering Review*, vol. 21, no. 5, pp. 49–51, 2001. [Online]. Available: <http://ieeexplore.ieee.org/document/4311362/>
- [23] EN 50160, "Standard EN 50160, voltage characteristics of electricity supplied by public electricity networks," 2010.
- [24] Y. J. Wang, "Analysis of effects of three-phase voltage unbalance on induction motors with emphasis on the angle of the complex voltage unbalance factor," *IEEE Transactions on Energy Conversion*, vol. 16, no. 3, pp. 270–275, 2001.
- [25] VDE-AR-N 4105, "Power generation systems connected to the LV distribution network." FNN, Tech. Rep., 2011.
- [26] J. Löfberg, "Yalmip: A toolbox for modeling and optimization in matlab," in *In Proceedings of the CACSD Conference*, Taipei, Taiwan, 2004.
- [27] I. Gurobi Optimization, "Gurobi optimizer reference manual," 2016. [Online]. Available: <http://www.gurobi.com>
- [28] K. Strunz, E. Abbasi, C. Abbey, C. Andrieu, F. Gao, T. Gaunt, A. Gole, N. Hatziaargyriou, and R. Iravani, "Benchmark Systems for Network Integration of Renewable and Distributed Energy Resources," *CIGRE, Task Force C6.04*, no. 273, pp. 4–6, 4 2014.